Excitons in molecular crystals from first-principles many-body perturbation theory: Picene versus pentacene

Pierluigi Cudazzo,[1] Matteo Gatti,[1] and Angel Rubio[1,2]

[1]*Nano-Bio Spectroscopy Group and ETSF Scientific Development Centre, Departamento Física de Materiales, Universidad del País Vasco UPV/EHU, Centro de Física de Materiales CSIC-UPV/EHU-MPC and DIPC, Avenida Tolosa 72, E-20018 San Sebastián, Spain*

[2]*Fritz-Haber-Institut der Max-Planck-Gesellschaft, Theory Department, Faradayweg 4-6, D-14195 Berlin-Dahlem, Germany*

(Received 1 August 2012; revised manuscript received 24 October 2012; published 7 November 2012)

By solving the first-principles many-body Bethe-Salpeter equation, we compare the optical properties of two prototype and technological relevant organic molecular crystals: picene and pentacene. Albeit very similar for the structural and electronic properties, picene and pentacene show remarkable differences in their optical spectra. While for pentacene the absorption onset is due to a charge-transfer exciton, in picene it is related to a strongly localized Frenkel exciton. The detailed comparison between the two materials allows us to discuss, on general grounds, how the interplay between the electronic band dispersion and the exchange electron-hole interaction plays a fundamental role in setting the nature of the exciton. It represents a clear example of the relevance of the competition between localization and delocalization in the description of two-particle electronic correlation.

DOI: 10.1103/PhysRevB.86.195307 PACS number(s): 78.40.Me, 71.35.Cc, 78.20.Bh

I. INTRODUCTION

Organic molecular crystals have been in the last years the focus of intense experimental and theoretical interest[1–5] for the large number of promising (opto)electronic applications, such as field-effect transistors, light-emitting diodes, or photovoltaic devices, just to mention a few examples. Nevertheless, there are still several fundamental open questions, concerning for example the mechanism of the charge transport (incoherent phonon-assisted hopping or coherent band transport)[6] or the nature of the lowest optical transition (weakly bound charge-transfer exciton or tightly bound Frenkel exciton).[7,8] The latter plays a crucial role in the applications of these materials in optoelectronic devices and will be the focus of the present work.

Organic molecular crystals consist of molecular units interacting through weak van der Waals forces. As a consequence, their electronic properties are mainly dictated by the electronic structure of the isolated molecules, which gives rise to nondispersive bands with π and σ character. Due to the strong localization of the electronic wave functions, the excited electron-hole (e-h) pairs tend to be confined to the single molecules. Thus, molecular solids are often considered a textbook example for the formation of Frenkel excitons with large binding energies.[9–12] However, if the dimension of the molecular units is large enough, the effective interaction for e-h pairs located on the same site or on two different sites becomes comparable. This leads to a competition between charge-transfer (CT) and Frenkel (FR) type excitons, even if the overlap between wave functions localized on different sites is negligible. Under these conditions, many-body effects become crucial for setting the character of the lowest-energy excitons and the optical properties of the molecular system. This makes molecular crystals interesting not only for the practical applications discussed above, but also as model systems for fundamental studies. In fact, the excitations in these systems can be described qualitatively, and often quantitatively, using simple models based on molecular orbitals.[9,10] In this way it is possible to identify and analyze in a transparent manner the role played by the different effects, such as exchange and direct e-h interactions or hopping processes, obtaining a clear and simple picture of the excitonic effects that is also valid for the description of other kinds of materials.

Although a large number of theoretical works have focused on the optical properties of molecular systems,[9,10] only recently the description of excitonic effects could be addressed using *ab initio* methods based on the solution of the Bethe-Salpeter equation (BSE) for the e-h Green's function.[13,14] Pioneering studies on oligomers of different type and size and on conjugated polymers (see, e.g., Refs. 15–24) have investigated, for instance, the effect of the crystal packing (also as a function of external pressure), the reduction of the exciton binding energy with the unit size, and the singlet-triplet splitting. On the experimental side, charge-transfer excitons, which often have small oscillator strength in conventional absorption spectra, could be identified using the Stark effect in electroabsorption spectroscopy.[25–27]

In the present work, by means of first-principles BSE calculations, we compare the optical properties of two isoelectronic aromatic molecular crystals: picene and pentacene. In both materials, the molecular units are made of five benzene rings, which in picene are joined in an armchair manner, while in pentacene they have a zigzag conformation (see Fig. 1). In the solid, the molecules are arranged in a herringbone structure, with two units per primitive cell, giving rise to a triclinic crystal structure in pentacene and to a monoclinic one in picene (see Fig. 1).[28,29] Pentacene belongs to the acene family, which is one of the most investigated families of organic crystals.[30,31] Picene has attracted a large interest very recently after the discovery of superconductivity with potassium doping.[32,33]

Here we demonstrate that although very similar for both electronic and structural properties, these two systems present remarkable differences in the absorption spectra. We show that while the low-energy region in pentacene is characterized by charge-transfer excitons,[7,15,17] in picene it is dominated by strongly bound Frenkel excitons. We relate the different behavior to the competition between direct and exchange e-h interactions, which becomes crucial in molecular crystals

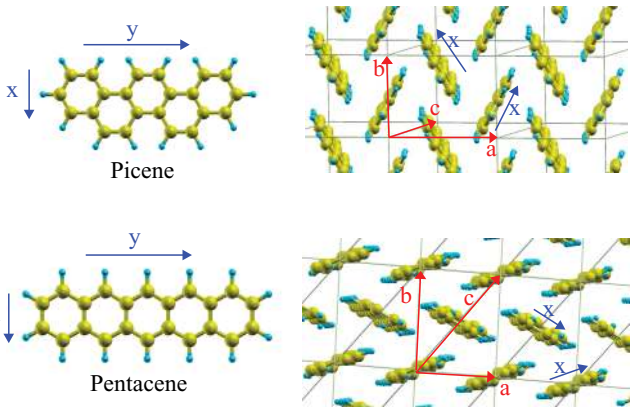

FIG. 1. (Color online) Molecular and crystal structure of picene and pentacene. We also indicate the shorter x and longer y molecular axes and their orientation with respect to the lattice vectors a, b, and c.

characterized by large aromatic molecular units. Finally, we discuss a simple and very general picture of many-body effects in this class of systems showing that the basic mechanism for the charge transfer is the interplay between exchange e-h interaction and band dispersion. This discussion allows us to elucidate the competition between localization and delocalization that is a key to understanding two-particle correlation effects in the materials.

II. THEORY

The Bethe-Salpeter equation in the Tamm-Dancoff approximation can be cast into an effective excitonic Hamiltonian (for an introduction to the theoretical framework see Ref. 14):

$$\hat{H}_{ex} = \sum_{c\mathbf{k}} \epsilon_{c\mathbf{k}} a^{\dagger}_{c\mathbf{k}} a_{c\mathbf{k}} - \sum_{v\mathbf{k}} \epsilon_{v\mathbf{k}} b^{\dagger}_{v\mathbf{k}} b_{v\mathbf{k}} + \sum_{vc\mathbf{k},v'c'\mathbf{k}'} \left(2\bar{v}^{vc\mathbf{k}}_{v'c'\mathbf{k}'} - W^{vc\mathbf{k}}_{v'c'\mathbf{k}'}\right) a^{\dagger}_{c\mathbf{k}} b^{\dagger}_{v\mathbf{k}} b_{v'\mathbf{k}'} a_{c'\mathbf{k}'}, \quad (1)$$

where v (c) is a valence (conduction) band, $\mathbf{k}$ is in the first Brillouin zone, and $a^{\dagger}$ (a) and $b^{\dagger}$ (b) are creation (annihilation) operators for electrons and holes, respectively. The quasiparticle (QP) energies, $\epsilon_{v\mathbf{k}}$ and $\epsilon_{c\mathbf{k}}$, are here obtained within Hedin's GW approximation (GWA),[34] as first-order perturbative corrections with respect to Kohn-Sham (KS) results in the local-density approximation (LDA). The BSE kernel is given by the sum of $2\bar{v}$, which includes only the short-range $\mathbf{G} \neq 0$ microscopic components of the bare Coulomb interaction v and the statically screened Coulomb interaction W. The matrix elements of $\bar{v}$ and W enter the BSE kernel as exchange and direct e-h interactions, respectively:

$$\bar{v}^{vc\mathbf{k}}_{v'c'\mathbf{k}'} = \langle c\mathbf{k}, v'\mathbf{k}'|\bar{v}|v\mathbf{k}, c'\mathbf{k}'\rangle, \quad (2)$$

$$W^{vc\mathbf{k}}_{v'c'\mathbf{k}'} = \langle c\mathbf{k}, v'\mathbf{k}'|W|c'\mathbf{k}', v\mathbf{k}\rangle. \quad (3)$$

The latter takes into account excitonic effects, while the former is responsible for crystal local-field effects (the factor 2 for $\bar{v}$ derives from the spin summation in the singlet channel). In this formalism, the optical spectra are obtained from the imaginary part of the macroscopic dielectric function, $\epsilon_2 = \mathrm{Im}\,\epsilon_M$, expressed in terms of the excitonic eigenenergies E^{λ} and eigenfunctions $|\Psi^{\lambda}\rangle = \sum_{vc\mathbf{k}} A^{\lambda}_{vc\mathbf{k}} a^{\dagger}_{c\mathbf{k}} b^{\dagger}_{v\mathbf{k}}|0\rangle$:

$$\epsilon_2(\omega) = \lim_{\mathbf{q}\to 0} \frac{8\pi}{q^2} \sum_{\lambda} \left| \sum_{vc\mathbf{k}} A^{\lambda}_{vc\mathbf{k}} \langle v\mathbf{k}+\mathbf{q}|e^{-i\mathbf{qr}}|c\mathbf{k}\rangle \right|^2 \delta(\omega - E^{\lambda}). \quad (4)$$

On a mathematical level, the diagonalization of the excitonic Hamiltonian (1) leads to the mixing of the different transitions between valence and conduction bands through the coefficients $A^{\lambda}_{vc\mathbf{k}}$, and the modification of the excitation energies E^{λ}.

In the following we present the calculated spectra obtained with three different levels of approximation: (i) setting $\bar{v} = W = 0$ in Eq. (1) corresponds to Fermi's golden rule within an independent-particle picture, where the spectrum (4) reduces to a sum over independent vertical transitions between bands calculated in the GWA; (ii) setting only $W = 0$ in Eq. (1) corresponds to the random-phase approximation (RPA), with the inclusion of crystal local-field effects (LFEs); (iii) the full solution of the BSE (1) allows also for the description of the excitonic effects, including bound excitons inside the QP band gap.

III. RESULTS

The spectra calculated[35] in the different approximations discussed in the previous section are summarized in Fig. 2 for pentacene and Fig. 3 for picene for polarizations along the three reciprocal lattice axes a^*, b^*, and c^*. For pentacene the calculated spectra are in agreement with those available in the literature,[15,17,18] the discrepancies being related to the different crystal structures adopted in the different calculations.

From the results obtained in the independent-particle picture [$\bar{v} = W = 0$ in Eq. (1)], it is clear that both picene

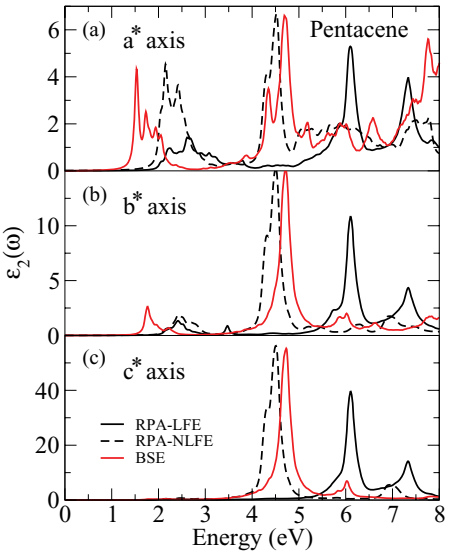

FIG. 2. (Color online) Absorption spectra of pentacene molecular crystal for different polarization directions: a^*, b^*, and c^*. The spectra are calculated with the following approximations: RPA without crystal local fields (RPA-NLFE) (black dashed lines), RPA with crystal local fields (RPA-LFE) (solid black lines), and full solution of the BSE (BSE) (red lines).

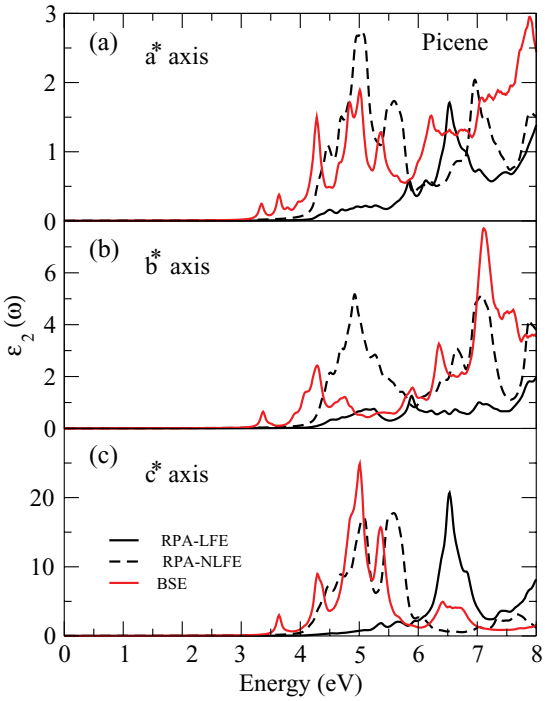

FIG. 3. (Color online) Same as Fig. 2 for picene.

and pentacene present strong anisotropic optical properties (see black dashed lines in Figs. 2 and 3). Picene and pentacene molecules belong to the C_{2v} and D_{2h} point group, respectively. Thus, by symmetry the only allowed transitions in the dipole approximation are $\pi \rightarrow \pi^*$ and $\sigma \rightarrow \sigma^*$ for polarization directions on the plane of the molecule and $\pi \rightarrow \sigma^*$ and $\sigma \rightarrow \pi^*$ for directions perpendicular to the molecular plane. In the condensed phase, due to the small overlap between wave functions localized on different sites, this picture is approximately still valid. The a^* and b^* axes have a large component normal to the xy plane of the molecule, while c^* is nearly parallel to the molecular main axis y (see Fig. 1). Therefore, in the low-energy region, where only $\pi \rightarrow \pi^*$ transitions are active, the oscillator strengths for light polarized in the a^*b^* plane have low intensities and the spectrum is dominated by transitions with polarizarion along c^*. However, in pentacene the transition between the highest occupied molecular orbital (HOMO) and the lowest unoccupied molecular orbital (LUMO) for a polarization parallel to the main axis y of the molecule is forbidden by symmetry. So also in the solid the absorption onset in pentacene has only contributions arising from transitions with polarization belonging to the a^*b^* plane, contrary to picene where the HOMO-LUMO transition is allowed. In the independent-particle picture, the onset corresponds to the *GW* band gap, which in picene[37] is 4.08 eV and in pentacene[15] is 2.02 eV. In both cases, the GWA corrects the underestimation of the band gaps in LDA, where they are 2.39 eV for picene and 0.67 eV for pentacene.

Beyond an independent-particle picture, we find that in both systems LFEs strongly affect the spectra (see solid black lines in Figs. 2 and 3). In fact, in both materials the electronic charge is strongly localized and polarizable, giving rise to an important Hartree response, which is responsible for LFEs through the matrix elements of the bare Coulomb interaction $\bar{v}$.[14] However, while in pentacene LFEs induce mainly a rigid blueshift of the spectrum, in picene LFEs lead also to a strong redistribution of the oscillator strength of the different features, modifying substantially the shape of the spectrum.

Finally, excitonic effects, which are taken into account through the full solution of the BSE, induce another remarkable redistribution of the oscillator strengths, counteracting LFEs (see red lines in Figs. 2 and 3). In both systems the resulting absorption spectrum is dominated by a large peak (located at 4.73 eV in pentacene and 5.00 eV in picene) related to a free exciton with polarization along the c^* axis. Moreover, e-h interactions give rise to several new structures inside the *GW* band gap (i.e., bound excitons). The calculated optical gap in picene is 3.34 eV and in pentacene is 1.53 eV. These values are in good agreement with results (3.3 eV for picene and 1.8 eV for a pentacene polymorph) from optical and electron-energy-loss experiments.[7,8,37,42,43]

The exciton binding energy, which is defined as the difference between the quasiparticle band gap and the peak position of the exciton, is hence larger in picene (0.7 eV) than in pentacene (0.5 eV), where for the higher polarizability the direct e-h interaction W is weaker than in picene. Both excitons are mainly related to HOMO-LUMO transitions. However while in pentacene the effect of higher energy transitions is negligible, in picene they give a remarkable contribution. In fact the exciton binding energy in picene evaluated including only HOMO-LUMO bands is 0.3 eV smaller than the value obtained from the full calculation. In both cases, several peaks corresponding to bound excitons are visible inside the QP gap (see Fig. 4). In picene the first three are located at 3.34, 3.37, and 3.64 eV and are visible for light polarized along the a^*, b^*, and c^* axis, respectively. In pentacene they have a remarkable oscillator strength only for light polarized in the a^*b^* plane and the first three are located at 1.53, 1.73, and 1.76 eV.

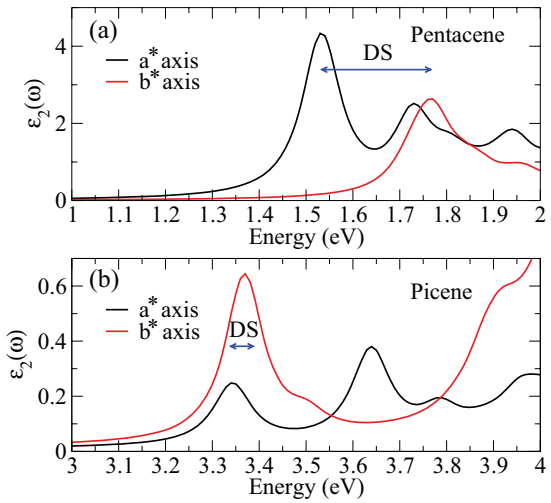

FIG. 4. (Color online) Bound excitons in pentacene (a) and picene (b) (the band gap in picene is 4.08 eV and in pentacene is 2.02 eV). The arrows indicate the Davydov splitting (DS). Note that the various structures in the spectra all have a pure electronic origin and do not derive from a coupling with vibrational excitations.

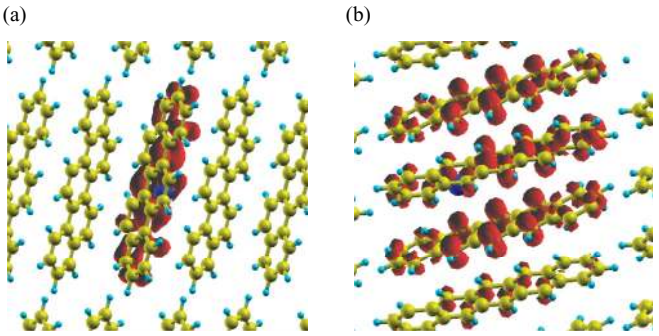

FIG. 5. (Color online) Electronic charge distribution $|\Psi^{\lambda}(\mathbf{r}_h,\mathbf{r}_e)|^2$ for a fixed position $\mathbf{r}_h$ of the hole (blue ball) for the lowest-energy singlet excitons in picene [panel (a)] and pentacene [panel (b)]. While in picene it is a Frenkel exciton, in pentacene it is a charge-transfer exciton. In ionic crystals for example, charge-transfer excitons arise from excitation from valence states localized around the anion to conduction states localized around the cation. On the contrary, in the present case note that valence and conduction wave functions are localized on both inequivalent molecules in the unit cell. Therefore, an exchange of the position of the hole between the two molecules would correspondingly exchange also the localization of the electronic charge distribution.

In Figs. 5(a) and 5(b) we draw the electronic charge distribution $|\Psi^{\lambda}(\mathbf{r}_h,\mathbf{r}_e)|^2$ for a fixed position of the hole $\mathbf{r}_h$, for the lowest-energy exciton in the two systems, which is visible only for light polarized along the a^* axis (see Fig. 4). We find that in the two systems this exciton has a different character. In pentacene it is a charge-transfer exciton: With respect to the position of the hole, the electronic charge is mainly localized on the nearest-neighbor molecules (see also Refs. 15, 16, and 18). In picene, instead, it is a Frenkel exciton with both the hole and electron charges mainly localized on the same molecule.

For the b^*-axis polarization the onset is given by a second exciton located at 1.76 eV in pentacene and 3.37 eV in picene (see Fig. 4). In both systems this exciton has the same character as the first one, i.e., a Frenkel exciton in picene and a charge-transfer exciton in pentacene, and mainly involves HOMO-LUMO states. Therefore we interpret the energy shift observed moving from the a^* to the b^* axis as the Davydov splitting[9] (DS) related to the first bound exciton. This splitting, which arises from the exchange e-h interaction, is peculiar to all molecular crystals made of pairs (or groups) of inequivalent molecules, oriented in some specific way one respect to the other. Thus, as in the present case, excitonic states that are symmetric and antisymmetric with respect to the exchange of an e-h pair between two nonequivalent molecules have different excitation energies.[9–11] We note that the DS is about 0.2 eV in pentacene, in good agreement with the experimental value[43] 0.15 eV, while in picene the DS is negligible: about one order of magnitude smaller. These observations suggest that in the two systems the DS has a different nature.

Finally, in addition to the lowest spin-singlet excitons, we consider also the lowest spin-triplet excitons that are dipole forbidden and thus not accessible in absorption experiments. To this end, we diagonalized the excitonic Hamiltonian (1) without exchange e-h interaction $2\bar{v}$. As for the singlet, also the lowest-energy triplet excitons involve mainly HOMO-LUMO transitions. Since the repulsive exchange e-h interaction $2\bar{v}$ is now missing, the triplet exciton is characterized by a higher binding energy: 1.3 eV for picene and 1.1 eV for pentacene. Moreover, in both systems it is a strongly localized Frenkel exciton, as can be inferred from Figs. 6(a) and 6(b). Therefore, the comparison between singlet and triplet excitons shows how the exchange e-h interaction plays a key role in setting the charge-transfer character of the singlet exciton that is experimentally visible in the absorption spectrum of pentacene.

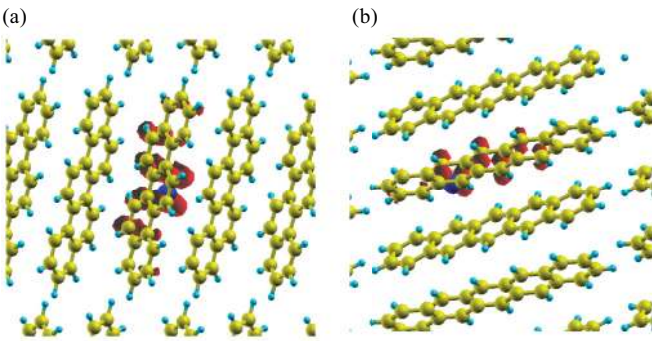

FIG. 6. (Color online) Same as Fig. 5 for the lowest-energy triplet excitons in picene [panel (a)] and pentacene [panel (b)]. It is a Frenkel exciton for both systems.

To summarize, from the comparison of the optical spectra in picene and pentacene crystals we have found that (i) in both systems the spectra are highly anisotropic as a consequence of the molecular character of the involved transitions; (ii) in both cases, crystal local-field and excitonic effects strongly modify the shape of the independent-particle spectra, with the creation of bound excitons inside the band gap; (iii) in picene the screening of the direct e-h interaction W is weaker, giving rise to excitons with larger binding energy than in pentacene; (iv) the lowest-energy excitons have different character: a Frenkel exciton for both spin singlet and spin triplet in picene, a charge-transfer exciton for spin singlet and a Frenkel exciton for spin triplet in pentacene—this shows that the exchange e-h interaction $\bar{v}$ plays a key role in the mechanism of the charge transfer exciton; (v) the Davydov splitting is much larger in pentacene than in picene and has a different nature in the two systems. In the following section we will present a physical explanation of these observations on the basis of a simple excitonic model.

IV. DISCUSSION

To better understand the excitonic effects in these systems, we rewrite the excitonic Hamiltonian (1) in a basis of wave functions localized on the molecular units, which in a first approximation are the wave functions of the isolated molecules:

$$\hat{H}_{ex} = \sum_{\mathbf{R}i,\mathbf{S}j} h^{e}_{\mathbf{R}i,\mathbf{S}j} a^{\dagger}_{\mathbf{R}i} a_{\mathbf{S}j} - \sum_{\mathbf{R}i,\mathbf{S}j} h^{h}_{\mathbf{R}i,\mathbf{S}j} b^{\dagger}_{\mathbf{R}i} b_{\mathbf{S}j} + \sum_{\mathbf{R}i,\mathbf{S}j,\mathbf{P}l,\mathbf{Q}m} \left(2\bar{v}^{\mathbf{S}j,\mathbf{P}l}_{\mathbf{Q}m,\mathbf{R}i} - W^{\mathbf{S}j,\mathbf{P}l}_{\mathbf{Q}m\mathbf{R}i}\right) a^{\dagger}_{\mathbf{R}i} b^{\dagger}_{\mathbf{Q}m} b_{\mathbf{S}j} a_{\mathbf{P}l}, \quad (5)$$

with

$$\bar{v}^{\mathbf{S}j,\mathbf{P}l}_{\mathbf{Q}m,\mathbf{R}i} = \langle c\mathbf{R}i, v\mathbf{S}j|\bar{v}|v\mathbf{Q}m, c\mathbf{P}l\rangle, \quad (6)$$

$$W^{\mathbf{S}j,\mathbf{P}l}_{\mathbf{Q}m\mathbf{R}i} = \langle c\mathbf{R}i, v\mathbf{S}j|W|c\mathbf{P}l, v\mathbf{Q}m\rangle. \quad (7)$$

Here the bold and thin letters indicate the lattice vectors and the molecular unit in the primitive cell, respectively. h^e is the single-particle Hamiltonian describing the motion of independent electrons: $h^e_{\mathbf{R}i,\mathbf{S}j} = \varepsilon^c\delta_{\mathbf{R}i,\mathbf{S}j} + t^c_{\mathbf{R}i,\mathbf{S}j}$, where ε^c is the electron level and t^c is the electron hopping integral. h^h is defined correspondingly for holes. $\Delta\epsilon = \varepsilon^c - \varepsilon^v$ is the HOMO-LUMO gap. From now on we drop the band index since we are interested in the lowest excitation that involves mainly the HOMO-LUMO states of the isolated molecule.

The excitonic wave function is written as a superposition of e-h pairs localized on different sites:[44]

$$|\Psi_{ex}\rangle = \sum_{\mathbf{R}} e^{i\mathbf{q}\cdot\mathbf{R}} \sum_{\mathbf{S}} \sum_{ij} C^{\mathbf{q}}_{\mathbf{S},ij} a^\dagger_{\mathbf{R}i} b^\dagger_{\mathbf{R}+\mathbf{S}j}|0\rangle, \quad (8)$$

where the coefficient $C^{\mathbf{q}}_{\mathbf{S},ij}$ are given by solution of the secular problem,

$$\langle 0|a_{\mathbf{R}i} b_{\mathbf{R}+\mathbf{S}j} e^{-i\mathbf{q}\cdot\mathbf{R}} \hat{H}_{ex}|\Psi_{ex}\rangle = E_{ex}(\mathbf{q}) C^{\mathbf{q}}_{\mathbf{S},ij}. \quad (9)$$

We neglect the overlap between wave functions localized on different molecules. Matrix elements of $\bar{v}$ are thus zero unless the condition $\mathbf{R}i = \mathbf{Q}m$ and $\mathbf{S}j = \mathbf{P}l$ is verified; that is, e-h pairs are on the same site. At the same time, matrix elements of W are not zero only when $\mathbf{R}i = \mathbf{P}l$ and $\mathbf{S}j = \mathbf{Q}m$, which means that an electron (or a hole) cannot scatter on a different site. The Hamiltonian (5) in this way becomes

$$\begin{aligned}\hat{H}_{ex} = &\sum_{\mathbf{R}i,\mathbf{S}j} h^e_{\mathbf{R}i,\mathbf{S}j} a^\dagger_{\mathbf{R}i} a_{\mathbf{S}j} - \sum_{\mathbf{R}i,\mathbf{S}j} h^h_{\mathbf{R}i,\mathbf{S}j} b^\dagger_{\mathbf{R}i} b_{\mathbf{S}j} \\ &+ \sum_{\mathbf{R}i,\mathbf{S}j} \left(2\bar{v}^{\mathbf{S}j,\mathbf{S}j}_{\mathbf{R}i,\mathbf{R}i} - \delta_{\mathbf{R}i,\mathbf{S}j} W^{\mathbf{S}j,\mathbf{S}j}_{\mathbf{R}i\mathbf{R}i}\right) a^\dagger_{\mathbf{R}i} b^\dagger_{\mathbf{R}i} b_{\mathbf{S}j} a_{\mathbf{S}j} \\ &+ \sum_{\mathbf{R}i,\mathbf{S}j} (1-\delta_{\mathbf{R}i,\mathbf{S}j}) W^{\mathbf{S}j,\mathbf{R}i}_{\mathbf{S}j\mathbf{R}i} a^\dagger_{\mathbf{R}i} b^\dagger_{\mathbf{S}j} b_{\mathbf{S}j} a_{\mathbf{R}i}. \quad (10)\end{aligned}$$

Here the third term describes the interaction between an electron and a hole localized on the same site. The fourth term instead describes the interaction between an electron and a hole on different sites. These two terms are coupled by the hopping terms (i.e., the first two), which are responsible for scattering processes of an electron (or a hole) from site to site.

In a first time we further neglect the hopping integrals in h^e and h^h that give rise to the finite dispersion of the bands. In this way, the excitonic Hamiltonian (10) decouples in two independent blocks $\hat{H}^{FR}_{ex}$ and $\hat{H}^{CT}_{ex}$, where the interacting parts $K_{ex} = 2\bar{v} - W$ are, respectively,

$$\hat{K}^{FR}_{ex} = \sum_{\mathbf{R}i,\mathbf{S}j} \left(2\bar{v}^{\mathbf{S}j,\mathbf{S}j}_{\mathbf{R}i,\mathbf{R}i} - \delta_{\mathbf{R}i,\mathbf{S}j} W^{\mathbf{S}j,\mathbf{S}j}_{\mathbf{R}i,\mathbf{R}i}\right) a^\dagger_{\mathbf{R}i} b^\dagger_{\mathbf{R}i} b_{\mathbf{S}j} a_{\mathbf{S}j}, \quad (11)$$

$$\hat{K}^{CT}_{ex} = \sum_{\mathbf{R}i,\mathbf{S}j} (1-\delta_{\mathbf{R}i,\mathbf{S}j}) W^{\mathbf{S}j,\mathbf{R}i}_{\mathbf{S}j,\mathbf{R}i} a^\dagger_{\mathbf{R}i} b^\dagger_{\mathbf{S}j} b_{\mathbf{S}j} a_{\mathbf{R}i}. \quad (12)$$

The first block gives rise to a Frenkel (FR) exciton with both electron and hole localized on the same site:

$$\left|\Psi^{FR}_{ex}\right\rangle = \sum_{\mathbf{R}i} e^{i\mathbf{q}\cdot\mathbf{R}} C^{\mathbf{q}}_{\mathbf{S}=0,ii} a^\dagger_{\mathbf{R}i} b^\dagger_{\mathbf{R}i}|0\rangle. \quad (13)$$

The second block, instead, produces a charge-transfer (CT) exciton with electron and hole localized on different sites:

$$\left|\Psi^{CT}_{ex}\right\rangle = \sum_{\mathbf{R}i,\mathbf{S}j} (1-\delta_{\mathbf{R}i,\mathbf{R}+\mathbf{S}j}) e^{i\mathbf{q}\cdot\mathbf{R}} C^{\mathbf{q}}_{\mathbf{S},ij} a^\dagger_{\mathbf{R}i} b^\dagger_{\mathbf{R}+\mathbf{S}j}|0\rangle. \quad (14)$$

In the triplet channel the exchange e-h interaction $\bar{v}$ is absent. Therefore, for the triplet both Hamiltonians $\hat{H}^{FR}_{ex}$ and $\hat{H}^{CT}_{ex}$ have only the direct e-h interaction W. However, as can be seen from Eqs. (11) and (12), while in the FR Hamiltonian the interacting e-h pairs are localized on the same molecule, in the CT they belong to different units. Thus, in general, the direct interaction W is always stronger in the FR Hamiltonian. As a consequence, this interaction being attractive, the lowest excited state in the triplet channel is always a FR excitation. On the other hand, in the singlet channel both solutions are in principle possible. In fact, in this case, while the CT Hamiltonian has only the direct e-h interaction W, the FR has both direct and exchange terms. Therefore, even if the direct e-h attraction is stronger for FR excitons, it is possible that, due to the presence of the repulsive exchange e-h interaction, the FR solution goes above the CT state.

In particular, for a system with two nonequivalent molecules in the unit cell, the secular problem of Eq. (9) for the FR Hamiltonian simplifies to the diagonalization of a 2×2 matrix with eigenvalues

$$E^{FR\pm}_{ex}(\mathbf{q}) = \Delta\epsilon + I(\mathbf{q}) - W \pm |J(\mathbf{q})|, \quad (15)$$

where $W = W^{\mathbf{R}i,\mathbf{R}i}_{\mathbf{R}i,\mathbf{R}i}$ is the on-site screened Coulomb interaction, and I and J are given by

$$I(\mathbf{q}) = 2\bar{v}^{\mathbf{R}i,\mathbf{R}i}_{\mathbf{R}i,\mathbf{R}i} + \sum_{\mathbf{R}'} 2\bar{v}^{\mathbf{R}'i,\mathbf{R}'i}_{\mathbf{R}i,\mathbf{R}i} e^{i\mathbf{q}\cdot\mathbf{R}'}, \quad (16)$$

$$J(\mathbf{q}) = \sum_{\mathbf{R}'} 2\bar{v}^{\mathbf{R}'j,\mathbf{R}'j}_{\mathbf{R}i,\mathbf{R}i;(i\neq j)} e^{i\mathbf{q}\cdot\mathbf{R}'}. \quad (17)$$

J and the last term in I are the excitation transfer interactions[12] (we assume that $\bar{v}^{\mathbf{R}'j,\mathbf{R}'j}_{\mathbf{R}i,\mathbf{R}i} = \bar{v}^{\mathbf{R}i,\mathbf{R}i}_{\mathbf{R}'j,\mathbf{R}'j}$). J is related to the scattering process of an e-h pair between two inequivalent molecules and, analogously, I between equivalent molecules in different unit cells. They are responsible for the dispersion of the FR exciton. The corresponding eigenstates at $\mathbf{q} = 0$ are symmetric, $|\Psi^{FR+}_{ex}\rangle$, and antisymmetric, $|\Psi^{FR-}_{ex}\rangle$, with respect to the exchange of the e-h pair between two nonequivalent molecules:

$$|\Psi^{FR\pm}_{ex}\rangle = a^\dagger_{\mathbf{R}1} b^\dagger_{\mathbf{R}1}|0\rangle \pm a^\dagger_{\mathbf{R}2} b^\dagger_{\mathbf{R}2}|0\rangle. \quad (18)$$

The energy difference $(E^{FR+}_{ex} - E^{FR-}_{ex})$ between symmetric and antisymmetric states is the Davydov splitting and is given by $2|J(\mathbf{q} = \mathbf{0})|$.

For the CT state, taking into account only the interaction between an electron and a hole on nearest neighbors and assuming that the corresponding matrix element is the same $\tilde{W}$ along all the directions, the secular problem in Eq. (9) is already in diagonal form with solution

$$E^{CT\pm}_{ex}(\mathbf{q}) = \Delta\epsilon - \tilde{W}. \quad (19)$$

This solution is at least twofold degenerate due to the lack of the exchange interaction that, through the Davydov splitting, removes the degeneracy between symmetric and antisymmetric states (extra degeneracy is related to the number

of nearest neighbors). Moreover, due to the lack of the exchange interaction, the CT exciton does not disperse.

Comparing the two solutions E_{ex}^{FR} and E_{ex}^{CT}, we note that in this simplified model the condition for the CT state to be the lowest-energy excitation is

$$I - W - |J| \geqslant -\tilde{W}. \tag{20}$$

In general, in molecular crystals made by small molecules this condition is not satisfied due to the large difference between W and $\tilde{W}$: The lowest excitation is thus a FR exciton. However, in aromatic molecular crystals where the size of the molecular units is large enough, the average e-h distances for an e-h pair on the same molecule or on two adjacent molecules are very close to each other so that W and $\tilde{W}$ become comparable. Under these conditions, if the repulsive contribution stemming from the exchange e-h interaction is strong enough, the condition in Eq. (20) is satisfied and the CT solution becomes energetically favorable.

Finally, the effect of the hopping integrals in the terms h^e and h^h in Eq. (5) is to mix CT and FR states.[5,10,45–49] Thus, in a real system with a nonzero band dispersion, the lowest excitation is always a mixture of the two solutions.

Taking into account only the hopping between nearest neighbors and treating it perturbatively, the correction to the energy level at $\mathbf{q} = 0$ is

$$\Delta E_{ex}^{\pm} \propto -\frac{(t^c \pm t^v)^2}{\left|E_{ex}^{FR\pm} - E_{ex}^{CT\pm}\right|}, \tag{21}$$

where t^c and t^v are the hopping integrals for conduction and valence bands, respectively. The energy correction and the mixing between CT and FR states get stronger for larger hoppings and for smaller energy difference between CT and FR states (see Fig. 7). We note that at $\mathbf{q} = 0$ the perturbation couples only states with the same symmetry and has different effects on the CT and FR states. When the lowest excited state is a FR exciton [Fig. 7(a)] (see, e.g., Ref. 45), the effect of the hopping is to reduce the Davydov splitting or, if strong enough, even to invert the order between the Davydov-split FR levels. On the other hand, when the lowest excited state is a CT exciton [Fig. 7(b)], the effect of the perturbation is to induce a Davydov splitting, which is absent in a pure CT state. Thus the Davydov splitting has different nature for CT and FR excitons. In general, we expect that it is smaller in FR states, since in this case it is related to the competition between the exchange e-h interaction J and the hopping term. Moreover the hopping is responsible for the dispersion of the CT exciton. While for FR states the dispersion is related to the exchange e-h interaction, in CT states it is mainly related to band-structure effects.

On the basis of this simple model, it is now possible to discuss the excitonic effect in picene and pentacene. First of all, we point out that in both systems, due to the nonzero band dispersion, the lowest excitation is always a mixture of FR and CT states.

Due to the strong localization of the excitonic wave function, it is clear that for the lowest-energy exciton in picene the effect of the hopping term is so small that the mixing with the CT state is negligible and the exciton preserves its Frenkel character [see Fig. 7(a)]. The main effect of the hopping is

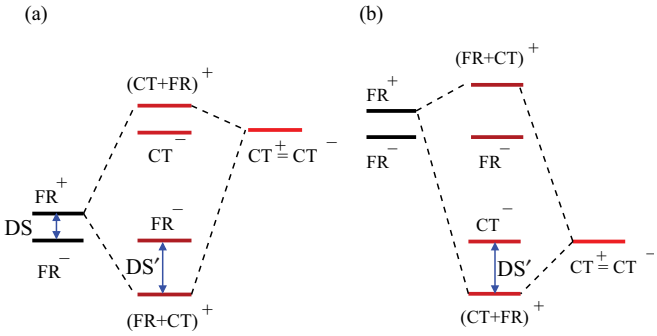

FIG. 7. (Color online) Energy-level diagram for the singlet channel showing the interaction between Frenkel (FR) and charge-transfer (CT) state when the lowest excitation is a Frenkel (a) or a charge-transfer (b) exciton. For simplicity, we assume that the hopping integrals for valence and conduction bands are the same ($t^v = t^c$). Thus antisymmetric states are not modified by the perturbation being in this case $\Delta E_{ex}^{-} \propto (t^c - t^v)^2 = 0$. $\mathrm{FR}^{\pm}$ and $\mathrm{CT}^{\pm}$ are the Frenkel and charge-transfer states in the absence of the hopping terms, while $(\mathrm{FR}+\mathrm{CT})^{+}$ and $(\mathrm{CT}+\mathrm{FR})^{+}$ are the mixture of Frenkel and charge-transfer states arising from the action of the hopping term on the FR^{+} and CT^{+} excitons, respectively. DS and DS′ are the Davydov splittings with and without the hopping term. Note that DS is zero in a pure charge-transfer state [panel (b)]. When the lowest excitation is a Frenkel exciton [panel (a)] mixing with CT exciton of the same symmetry can in principle (for large values of the hopping term) cause a shift of the symmetric state $(\mathrm{FR}+\mathrm{CT})^{+}$ below the antisymmetric state FR^{-}, as shown in panel (a).

to reduce the Davydov splitting. Thus, as expected for a pure FR exciton, the lowest excited state has an antisymmetric FR^{-} character.

On the other hand, the strong FR-CT mixing in pentacene is due to the smaller difference between the FR and CT solutions and to the larger value of the hopping integrals. In fact, the widths of pentacene and picene LUMO-derived bands are 0.96 and 0.27 eV, respectively (they are 0.77 and 0.72 eV for the HOMO-derived bands). And, since $\tilde{W}$ is more similar to W, the difference between FR and CT (which is given by $I - J + \tilde{W} - W$) is strongly reduced in pentacene. Thus, the effects of the exchange interaction are more relevant than in picene. Therefore, from our simple model we can conclude that the charge-transfer character of the exciton in pentacene arises from the interplay between the exchange e-h interaction and the band dispersion that makes the hopping term large enough to cause a strong mixing between FR and CT states. In particular, it shifts the mixed symmetric state below the antisymmetric one,[54] with a Davydov splitting about one order of magnitude larger than in picene and with opposite sign.

Our results for pentacene are in good agreement with previous *ab initio* theoretical works.[15,17] However, they seem to be in contrast with the traditional interpretation of the electroabsorption experiments,[25] which suggests that the lowest excited state in pentacene is a FR exciton. The electroabsorption signal has different behavior for FR and CT states. Its shape thus identifies unequivocally the exciton character when this is a pure FR or CT state. However, the interpretation of the electroabsorption spectra is rather complicated in real materials where the excitons are always

a mixture of the two configurations.[48–53] In order to settle definitely this issue, a first-principles BSE calculation of the electroabsorption spectra would be very useful, which at the moment is unfortunately not possible.

Finally, also the anisotropy of the absorption spectra and their behavior moving from the a^* to the b^* axis can be interpreted in terms of a molecular picture.[9] Here we call $\hat{\mathbf{x}}$ and $\hat{\mathbf{y}}$ the dipole matrix elements for the HOMO-LUMO transition of the isolated molecule for the direction parallel to the x and to the y axis, respectively (see Fig. 1). The dipole matrix element for the optical transition corresponding to the FR exciton in picene can be calculated as

$$\langle \Psi^{FR\pm} | \mathbf{r} | 0 \rangle = (\alpha_A \pm \alpha_B)\hat{\mathbf{x}} + (\beta_A \pm \beta_B)\hat{\mathbf{y}}, \qquad (22)$$

where α_A and β_A are the projections of $\mathbf{r}$ along the x and y axes of the molecule A (and, analogously, α_B and β_B for the molecule B). From the orientation of the two molecules A and B in the unit cell of the crystal, we find that in picene β_A and β_B have always the same sign. Moreover $\alpha_A = -\alpha_B$ for the dipole moment along a^* and $\alpha_A = \alpha_B$ along b^*. Thus the antisymmetric FR^- state is visible only along the a^* axis, while the symmetric FR^+ state is in principle visible along both directions a^* and b^*. However, the two molecules are oriented in such a way that the y axis is nearly perpendicular to the a^*b^* plane. Hence $|\beta_A|$ and $|\beta_B| \approx 0$ and this explains why the symmetric and antisymmetric states are visible only along the b^* and a^* axes, respectively.

If we neglect dipole matrix elements between wave functions localized on different molecules, we can still describe the optical spectra of pentacene in terms of Eq. (22), although in this case the excitonic wave function is delocalized on different molecules. In the present case, due to the orientation of the molecules (see Fig. 1), $\alpha_A = \alpha_B$ for the dipole moment along a^* and $\alpha_A = -\alpha_B$ along b^*. Moreover due to the symmetry of the pentacene molecule $\hat{\mathbf{y}}$ is zero so that the symmetric and antisymmetric states are visible only along the a^* and b^* axes, respectively.

V. CONCLUSIONS

To summarize, we have compared the optical properties of two similar organic molecular crystals, picene and pentacene. On the basis of an *ab initio* Bethe-Salpeter calculation, we have found that while the lowest-energy singlet exciton in pentacene has a weakly bound charge-transfer character, in picene it is a tightly bound Frenkel exciton. We have also discussed the different origin of the Davydov splitting in the two materials, together with the anisotropy of the absorption spectra.

The comparison between picene and pentacene has served as a model study to elucidate the interplay between the attractive direct and the repulsive exchange electron-hole interactions, and the effect of the hopping integrals. This discussion has a general validity and is useful to understand the result of the competition between localization and delocalization for the two-particle electronic correlation, which determines the optical properties of the materials.

ACKNOWLEDGMENTS

We thank Francesco Sottile for fruitful discussions. We acknowledge financial support from the European Research Council Advanced Grant DYNamo (ERC-2010-AdG, Proposal No. 267374), Spanish Grants No. FIS2011-65702-C02-01 and No. PIB2010US-00652, ACI-Promociona (ACI2009-1036), Grupos Consolidados UPV/EHU del Gobierno Vasco (IT-319-07), Consolider nanoTHERM (Grant No. CSD2010-00044), and European Commission project CRONOS (280879-2 CRONOS CP-FP7). Computational time was granted by i2basque and BSC "Red Española de Supercomputacion."

[1] S. R. Forrest, Nature (London) **428**, 911 (2004).
[2] T. W. Kelley, P. F. Baude, Ch. Gerlach, D. E. Ender, D. Muyres, M. A. Haase, D. E. Vogel, and S. D. Theiss, Chem. Mater. **16**, 4413 (2004).
[3] G. Li, V. Shrotriya, J. Huang, Y. Yao, T. Moriarty, K. Emery, and Y. Yang, Nat. Mater. **4**, 864 (2005).
[4] A. Facchetti, Mater. Today **10**, 28 (2007).
[5] V. M. Agranovich and G. F. Bassani, *Thin Films and Nanostructures: Electronic Excitations in Organic Based Nanostructures* (Elsevier Academic Press, Amsterdam, 2003).
[6] F. Ortmann, F. Bechstedt, and K. Hannewald, New J. Phys. **12**, 023011 (2010).
[7] R. Schuster, M. Knupfer, and H. Berger, Phys. Rev. Lett. **98**, 037402 (2007).
[8] F. Roth, R. Schuster, A. König, M. Knupfer, and H. Berger, J. Chem. Phys. **136**, 204708 (2012).
[9] A. S. Davydov, *Theory of Molecular Excitons* (McGraw-Hill, New York, 1962).
[10] V. M. Agranovich, *Excitations in Organic Solids* (Oxford University Press, Oxford, 2008).
[11] R. S. Knox, *Theory of Excitons* (Academic Press, New York, 1963).
[12] F. Bassani and G. Pastori Parravicini, *Electronic States and Optical Transitions in Solids* (Pergamon Press, Oxford, 1975).
[13] S. Albrecht, L. Reining, R. Del Sole, and G. Onida, Phys. Rev. Lett. **80**, 4510 (1998); L. X. Benedict, E. L. Shirley, and R. B. Bohn, *ibid.* **80**, 4514 (1998); M. Rohlfing and S. G. Louie, Phys. Rev. B **62**, 4927 (2000).
[14] G. Onida, L. Reining, and A. Rubio, Rev. Mod. Phys. **74**, 601 (2002), and references therein.
[15] M. L. Tiago, J. E. Northrup, and S. G. Louie, Phys. Rev. B **67**, 115212 (2003).
[16] K. Hummer, P. Puschnig, and C. Ambrosch-Draxl, Phys. Rev. Lett. **92**, 147402 (2004).
[17] K. Hummer and C. Ambrosch-Draxl, Phys. Rev. B **71**, 081202(R) (2005); **72**, 205205 (2005).
[18] C. Ambrosch-Draxl, D. Nabok, P. Puschnig, and Ch. Meisenbichler, New J. Phys. **11**, 125010 (2009).
[19] N. Sai, M. L. Tiago, J. R. Chelikowsky, and F. A. Reboredo, Phys. Rev. B **77**, 161306 (2008).

[20]L. Zoppi, L. Martin-Samos, and K. K. Baldridge, J. Am. Chem. Soc. **133**, 14002 (2011).
[21]J. W. van der Horst, P. A. Bobbert, M. A. J. Michels, G. Brocks, and P. J. Kelly, Phys. Rev. Lett. **83**, 4413 (1999).
[22]A. Ruini, M. J. Caldas, G. Bussi, and E. Molinari, Phys. Rev. Lett. **88**, 206403 (2002).
[23]P. Puschnig and C. Ambrosch-Draxl, Phys. Rev. Lett. **89**, 056405 (2002).
[24]M. L. Tiago, M. Rohlfing, and S. G. Louie, Phys. Rev. B **70**, 193204 (2004).
[25]L. Sebastian, G. Weiser, and H. Bässler, Chem. Phys. **61**, 125 (1981).
[26]L. Sebastian, G. Weiser, G. Peter, and H. Bässler, Chem. Phys. **75**, 103 (1983).
[27]Z. Shen, P. E. Burrows, S. R. Forrest, M. Ziari, and W. H. Steier, Chem. Phys. Lett. **236**, 129 (1995).
[28]Ch. C. Mattheus, A. B. Dros, J. Baas, G. T. Oostergetel, A. Meetsma, J. L. de Boer, and T. T. M. Palstra, Acta Crystallogr. C **57**, 939 (2001).
[29]A. De, R. Ghosh, S. Roychowdhury, and P. Roychowdhury, Acta Crystallogr. C **41**, 907 (1985).
[30]M. Bendikov, F. Wudl, and D. F. Perepichka, Chem. Rev. **104**, 4891 (2004).
[31]J. E. Anthony, Angew. Chem. Int. Ed. **47**, 452 (2008).
[32]R. Mitsuhashi, Y. Suzuki, Y. Yamanari, H. Mitamura, T. Kambe, N. Ikeda, H. Okamoto, A. Fujiwara, M. Yamaji, N. Kawasaki, Y. Maniwa, and Y. Kubozono, Nature (London) **464**, 76 (2010).
[33]Y. Kubozono, H. Mitamura, X. Lee, X. He, Y. Yamanari, Y. Takahashi, Y. Suzuki, Y. Kaji, R. Eguchi, K. Akaike, T. Kambe, H. Okamoto, A. Fujiwara, T. Kato, T. Kosugi, and H. Aoki, Phys. Chem. Chem. Phys. **13**, 16476 (2011).
[34]L. Hedin, Phys. Rev. **139**, A796 (1965).
[35]We have adopted the experimental crystal structures of Refs. 29 and 36. Ground-state and *GW* band-structure calculations have followed those in Refs. 37 and 38. The absorption spectra have been obtained with a $6 \times 6 \times 4$ grid of **k** points and 53 occupied and 29 empty bands. For the matrix elements of the BSE kernel 400 **G** vectors have been used in the sums. *GW* energies have been explicitly calculated for all the bands and **k** points, without using a scissors correction to LDA results. We have verified that coupling between resonant and antiresonant transitions, beyond the Tamm-Dancoff approximation that has been adopted here, does not modify significantly the absorption onset, in agreement with Ref. 18. We have used the following codes: ABINIT (Ref. 39), YAMBO (Ref. 40), and EXC (Ref. 41).
[36]O. D. Jurchescu, Ph. D. thesis, Rijksuniversiteit Groningen, The Netherlands, 2006, http://dissertations.ub.rug.nl/faculties/science/2006/o.d.jurchescu.
[37]F. Roth, M. Gatti, P. Cudazzo, M. Grobosch, B. Mahns, B. Büchner, A. Rubio, and M. Knupfer, New J. Phys. **12**, 103036 (2010).
[38]P. Cudazzo, M. Gatti, F. Roth, B. Mahns, M. Knupfer, and A. Rubio, Phys. Rev. B **84**, 155118 (2011).
[39]X. Gonze, G.-M. Rignanese, M. Verstraete, J.-M. Beuken, Y. Pouillon, R. Caracas, F. Jollet, M. Torrent, G. Zerah, M. Mikami, Ph. Ghosez, M. Veithen, J.-Y. Raty, V. Olevano, F. Bruneval, L. Reining, R. Godby, G. Onida, D. R. Hamann, and D. C. Allan, Z. Kristallogr. **220**, 558 (2005).
[40]A. Marini, C. Hogan, M. Grüning, and D. Varsano, Comput. Phys. Commun. **180**, 1392 (2009).
[41]The EXC code is developed by the French node of the ETSF; see http://www.bethe-salpeter.org.
[42]F. Roth, B. Mahns, B. Büchner, and M. Knupfer, Phys. Rev. B **83**, 165436 (2011).
[43]M. Dressel, B. Gompf, D. Faltermeier, A. K. Tripathi, J. Pflaum, and M. Schubert, Opt. Express **16**, 19770 (2008); D. Faltermeier, B. Gompf, M. Dressel, A. K. Tripathi, and J. Pflaum, Phys. Rev. B **74**, 125416 (2006).
[44]E. L. Shirley, L. X. Benedict, and S. G. Louie, Phys. Rev. B **54**, 10970 (1996).
[45]H. Yamagata, J. Norton, E. Hontz, Y. Olivier, D. Beljonne, J. L. Brédas, R. J. Silbey, and F. C. Spano, J. Chem. Phys. **134**, 204703 (2011).
[46]M. Hoffmann, K. Schmidt, T. Fritz, T. Hasche, V. M. Agranovich, and K. Leo, Chem. Phys. **258**, 73 (2000).
[47]A.-M. Janner, R. Eder, B. Koopmans, H. T. Jonkman, and G. A. Sawatzky, Phys. Rev. B **52**, 17158 (1995).
[48]P. Petelenz, M. Slawik, K. Yokoi, and M. Z. Zgierski, J. Chem. Phys. **105**, 4427 (1996).
[49]P. Petelenz, B. Petelenz, H. F. Shurvell, and V. H. Smith, Jr., Chem. Phys. **119**, 25 (1988).
[50]M. Slawik and P. Petelenz, J. Chem. Phys. **107**, 7114 (1997).
[51]M. Slawik and P. Petelenz, J. Chem. Phys. **111**, 7576 (1999).
[52]M. Andrzejak, P. Petelenz, and M. Slawik, J. Chem. Phys. **117**, 1328 (2002).
[53]G. Mazur, P. Petelenz, and M. Slawik, J. Chem. Phys. **118**, 1423 (2003).
[54]Note that although both $(\mathrm{FR}+\mathrm{CT})^+$ and $(\mathrm{CT}+\mathrm{FR})^+$ configurations (see Fig. 7) are in principle possible, in models based on molecular orbitals (see, e.g., Refs. 5, 10, 45–48) the $(\mathrm{FR}+\mathrm{CT})^+$ configuration is energetically preferred to the $(\mathrm{CT}+\mathrm{FR})^+$ one.